6

Basics and Biomedical Applications of Dielectric Barrier Discharge (DBD)

Nikita Bibinov[1], Priyadarshini Rajasekaran[1], Philipp Mertmann[1]
Dirk Wandke[2], Wolfgang Viöl[3,4] and Peter Awakowicz[1]
[1]*Institute for Electrical Engineering and Plasma Technology, Ruhr-Universität Bochum*
[2]*Cinogy GmbH, Duderstadt*
[3]*University of Applied Sciences and Arts, Göttingen*
[4]*Laser Laboratory Göttingen*
Germany

1. Introduction

Plasmas are partially ionized gases and are described as the "fourth state" of matter. Irving Langmuir coined the word 'plasma', in 1928, for the ionized gas in which electrons, ions, and excited particles are suspended similar to the cells suspended in the blood plasma. Naturally-existing plasma includes the sun and the stars, lightening, polar lights, etc. Artificially-produced plasmas are fluorescent lamps, neon signs, plasma displays and monitors, etc. Much more applications of plasma have been made possible in the recent decades.

There are several methods for plasma generation. One among them is by applying sufficient electric field in different gas mixtures confined in a low-pressure chamber. Such low-pressure plasmas are suitable for tailoring the surface properties of different materials, for film deposition, for sterilization of non-living matter, etc. However, treatment of pressure-sensitive objects and materials is not possible using a low-pressure system. Treatment of living tissues, as in the case of medical treatment, is possible only with plasma devices which operate at atmospheric pressure.

Because of high pressure, discharge ignition at atmospheric conditions requires high voltage and can arouse high current density. The gas temperature in active plasma volume increases up to several thousand degrees. By such treatment, the living object is over heated (hyperthermia) and partially evaporated. Such plasma sources are used in surgery as plasma scalpel and blood coagulator (Stoffels, 2007).

For gentle treatment of living object at atmospheric pressure conditions, limitation of current flowing through the treated object is necessary. This can be achieved by placing the object slightly away from the active plasma volume as in the case of "indirect" plasma treatment. The other ways are short voltage pulsing (Ayan, 2008 & Walsh, 2008) and using a dielectric barrier (otherwise called 'insulator') that drastically reduces electric current through the treated object. Devices using the latter are so-called "dielectric barrier discharges (DBD)" which are useful for "direct" treatment of living object which comes in immediate contact with the plasma.

DBDs comprise of a pair of electrodes, separated by a small gap filled with a gas. When the electrodes are energized by a high voltage – high enough that the gas starts conducting, the 'breakdown' condition has been achieved. After breakdown, the gas permits current flow across the electrodes and completes the electric circuit. Usually DBD operates by AC voltage with amplitude of about 10-20 kV and frequency of 10-100 kHz. The averaged current amounts from few up to several tens of milliamps. DBDs have broad field of applications like in ozonators, air and water purification, etc. (Kogelschatz, 2003). The gas is ionized resulting in the formation of free electrons and positive ions. Free electrons are accelerated by the electric field in the gas gap and ionise neutral gas molecules by impact resulting in an electron avalanche. Neutral atoms can also be excited by electron impact. Part of these excited gas atoms and molecules relax to their ground levels through the emission of photons at a certain wavelength. This attributes to plasmas of different colours. The chemically-active radicals and long living (so-called "metastable") excited atomic and molecular species can also be produced during relaxation. This makes plasma chemically active by interaction with surrounding gas and solid body surfaces.

DBD can operate in both filamentary and homogeneous modes depending on the plasma conditions. The former consists of thin plasma channels stochastically distributed (i.e. spatially and temporally) in the gap between the working electrodes. The latter, so-called atmospheric pressure glow discharge (APGD), fills the entire gap with practically homogeneous (or uniform) plasma during short discharge pulse. DBD is a "cold" plasma where electron temperature (T_e) is about 23000 K ($kT_e \sim 2$ eV, where "k" is Boltzmann constant) which is higher than the gas temperature (400-500 K) in the short-living plasma channel as well as the surrounding gas temperature (about 300 K).

For gentle treatment of living tissues, both "indirect" and "direct" plasma treatments can be applied. In the former case, the living object is treated "indirectly" by flux of chemically-active atoms and radicals - which are produced in active plasma volume of the plasma source, and are transported to the treated object as an effluent by the gas flow. During transport to the treated object, the chemical composition of the effluent is changed because of chemical reactions of atoms and radicals among themselves as well as with the surrounding gas. Quantity of short-living radicals reaching the treated surface is low in indirect plasma treatment. By "direct" plasma treatment, the living object itself serves as one of the electrode as for the DBD, and the active species are produced directly near the treated surface and the short-living radicals can reach the object instantly. During "direct" plasma treatment the living object is heated, is bombarded by neutral and ionized species, and conducts electric current. The role played by the object itself during treatment is more complicated and less is known but obviously offers a big potential for applications like healing of different skin diseases. This has raised interest among different working groups to develop plasma devices that can be used for medical treatment of human body.

The first and foremost will be the study of response and influence of living objects on plasma treatment, and then the optimisation of the treatment process which requires the determination of fluxes of photons, electrons, atomic and molecular species on the treated surface. For this purpose, we apply a combination of experimental and theoretical methods for plasma characterisation which are otherwise not ideal individually and hence, when used together give reliable and valid information useful for optimization of plasma treatment.

The object of our study is to optimize a DBD for "direct" treatment of surface of human body facilitating therapeutic use of the DBD in dermatology and other medical applications (Fridman, 2008).

2. Dielectric Barrier Discharge (DBD)

Generally, DBDs comprise of two parallel or concentric electrodes connected to a high voltage power supply. The gap between electrodes amounts usually about 1-2 mm. Pulsed or AC high voltage with frequency from 50 Hz up to several 100 kHz can be applied. DBDs can be operated with different gases namely, nitrogen, oxygen, rare gases, etc. To limit the electric current between the electrodes and to avoid the formation of current arcs, atleast one of the electrodes is covered with a dielectric material namely quartz, ceramic, etc.
DBDs for medical use comprise of only one electrode which is covered with a dielectric. When supplied with a high voltage, these devices are able to generate plasma at close vicinity to the human body. In this case, the human body itself acts as the counter electrode and the plasma is generated in air in the gap between the dielectric-covered electrode and the body. This means that the applied voltage should be selected in such a way to generate plasma in air at atmospheric-pressure and more importantly, in the small gap between the working electrode and the body.

2.1 DBD in air

DBD operated in air is characterized, usually, by the formation of filament-like structures called "microdischarges". Microdischarges occur stochastically-distributed in the gap between the electrodes. These microdischarges are several tens of microns in diameter and last for several tens of nanoseconds. The electron density in microdischarges is very high and, therefore, excitation and dissociation of nitrogen and oxygen molecules during electron impact take place abundantly.
Plasma-aided chemical reactions in air contribute to complex air-plasma chemistry. Nitrogen and oxygen molecules in air are effectively excited and dissociated by the energetic electrons, resulting in the synthesis of nitric oxide (NO), ozone (O_3) and several other reactive species. Photons are emitted, in the ultra-violet (UV) range, during the relaxation of excited N_2 and NO molecules in the plasma. These chemically-active species and radiation are useful for several biomedical applications. NO, ozone and UV radiation are useful for promoting healing of chronic wounds and skin ulcers (Fridman, 2008). The anti-microbial effect of ozone and UV is used in purification of potable water (Kogelschatz, 2003 & Legrini, 1993). The same effect can also be exploited for disinfection/sterilization of skin surface through plasma treatment. Hence, air-plasma treatment can be used to disinfect wounds as well as the surrounding tissues (Boudam, 2006).

2.2 Optimization of plasma treatment of human body

Optimizing the DBD device for bio-medical application requires progressive investigation through plasma characterizations and appropriate biological studies. Plasma characterization allows for understanding the plasma parameters (namely electron distribution function and electron density) and gas temperature while biological tests are helpful to ascertain the 'safe doses' of chemically-active particles and photons. In addition, equipments which will be subjected to use on human body requires clinical trials involving people. Prior to such clinical trials, the device has to well- investigated to gain insight of the characteristics of the plasma produced by the device. Prior to using the device on human body and characterizing the plasma, small animals and simple electrodes of different materials like metals (Kuchenbecker, 2009), glass and liquid medium (Rajasekaran, 2010) are subjected to plasma treatment to gain insight into the respective plasma conditions and

thereby deduce the response of the treated object which can be helpful for optimization of the plasma device for medical applications.

3. Plasma characterization

To optimize the treatment conditions, the fluxes of chemically-active species to the surface of the treated object must be studied for which the chemical kinetics in plasma volume must be simulated. Information and values of gas temperature, electron distribution function and electron density are necessary for simulation. Concentration of gas molecules (or atoms, otherwise) and rate constants of chemical reactions are dependent on the gas temperature. The chemically-active species are produced by electron impact and therefore electron distribution function and electron density are necessary for determination of electron-impact excitation and dissociation rate of molecules.

We refer the term 'plasma characterization' to the method of determination of gas temperature (T_g) and plasma parameters namely, electron density (n_e) and electron velocity distribution function (EVDF).

3.1 Gas temperature (T_g)

Gas temperature in microdischarges of DBD differs strongly from that of surrounding gas and chemical reactions occur at different gas temperature. Therefore, for reliable simulation of chemical kinetics, the gas temperature in active plasma volume and in afterglow phase*, must be determined.

With reference to the filamentary and homogeneous modes of the DBD, when discharge is ignited in air gap between electrodes for short time (several ns), the gas temperature can reach values of 400-500 K in the filamentary discharge mode (Rajasekaran, 2009) and close to 300 K in the homogenous discharge mode (Rajasekaran, 2010). In the afterglow phase, gas temperature in the filament and in the surrounding volume decreases rapidly because of thermo-conductivity.

3.2 Electron density (n_e)

Electron density in DBD in air differs strongly in both discharge modes. In homogeneous DBD, electron density amounts to about 10^{17} m^{-3} (Rajasekaran, 2010). But in the microdischarge of the filamentary mode, electron density reaches 10^{20} – 10^{21} m^{-3} (Rajasekaran, 2009). Plasma is quasi-neutral and density of positive ions is approximately equal to the electron density. During collisions of neutral species with ions-accelerated in electric field, gas in the filament is heated up to 500 K and sometimes even more (Kuchenbecker, 2009). Electric field in the DBD channel in air is sufficient for supporting the discharge for only several nanoseconds. After that, because of charge of dielectric surface, electric field in the air gap decreases and discharge is interrupted.

3.3 Electron Velocity Distribution Function (EVDF)

Electrons are produced in the air gap during secondary emission (bombardment of cathode by positive ions) and during gas ionisation in the plasma volume by electron impact. The electrons are accelerated by the electric field in discharge gap and lose kinetic energy during

* Afterglow phase refers to the state after the microdischarge has extinguished.

inelastic collisions with atoms and molecules. To describe conditions and properties of electron gas, the electron distribution function (f) is employed. The electron distribution function can be simulated by solving Boltzmann equation (1):

$$\frac{\partial f}{\partial t} + \nabla_r f - \nabla_v \left(\frac{e}{m_e}\vec{E} f\right) = S_{coll}, \quad (1)$$

where, e - elementary charge;
m_e - electron mass;
∇ - *nabla*-differential operator denotes gradient in phase space;
$\vec{E}$ - electric field; and
S_{coll} - collision term which comprises of all kinds of binary electron-heavy particle collisions.

The Boltzmann equation is a continuity equation for distribution function in the phase space. It describes the temporal evolution of f in the co-ordinate space (second term in equation (1)) and in velocity space (third term in equation (1)). The flux in coordinate space is caused by density gradients. A flux in velocity space results from the action of electrostatic force.

The electron distribution functions in plasma can be presented in two different ways: Electron Energy Distribution Function (EEDF or $f_E(E)$) and Electron Velocity Distribution Function (EVDF or $f_v(E)$) (Bibinov, 2005). Both have different units and are differently normalised. In plasma characterisation, we determine EVDF (in $eV^{-3/2}$) applying Optical Emission Spectroscopy (OES).

4. Diagnostics methods

For plasma characterization at low pressure conditions, a Langmuir probe can be applied. Using voltage-current characteristics of the electric probe, plasma potential, electron distribution function and electron density can be determined (Lieberman, 1994). For various reasons, electron distribution function can be determined usually in electron kinetic energy region up to about 10 eV (Godyak, 1992 & Bibinov, 2008). For calculation of dissociation and excitation rates under electron impact, distribution function in broader kinetic energy region is essential. Furthermore, electric probe cannot be applied for characterisation of atmospheric pressure DBD in air because of very small plasma volume and short plasma pulse duration.

Optical emission spectroscopy (OES) is the second method, which can give information concerning EVDF in plasma. In OES, the emission due to relaxation of excited molecules and ions in the plasma is measured using a spectrometer which is then used to determine EVDF by fitting procedure. Electronic excited states of atoms and molecules are excited during impact of electrons with kinetic energy higher than 10 eV. Therefore, OES diagnostics can be used for determination of EVDF in electron kinetic energy range higher than 10 eV. Combination of probe and OES diagnostics provides EVDF in broad electron kinetic energy range and can be used for characterisation of low pressure plasmas also (Bibinov, 1998 & Bibinov, 2008).

4.1 OES diagnostics of DBD in air

Photoemission of atoms and molecules can be used for the purpose of OES diagnostics of DBD in air. For this, intensities of molecular emissions bands and atomic lines must be

measured in absolute units and mechanism of their excitation must be explicitly known. Emission spectrum (see fig. 1) of discharge in air consists mainly the emission bands of nitrogen and nitric oxide.

The two nitrogen molecular bands ("second positive" system N_2(C-B) and "first negative" system N_2^+(B-X)) which are excited by electron impact of the ground state of nitrogen molecule are observed in the emission spectrum of air plasmas at atmospheric pressure and can be used for plasma characterisation. The NO(A-X) bands detected in the UV-C region (λ < 280 nm) are excited from the ground state of nitric oxide, density of which is not known *a priori* and cannot be used for plasma characterisation.

The gas temperature in the active plasma volume is determined by comparison of measured and simulated spectra of nitrogen molecule N_2(C-B,0-0). Because of high efficiency of rotational relaxation at atmospheric pressure conditions, the temperature of rotational and translational degrees of freedom of excited neutral nitrogen molecules are equal. We simulate N_2(C-B,0-0) molecular band with variated rotational temperature and compare these spectra with measured ones (fig.2). The rotational temperature (that is equal to the gas temperature) in active plasma volume are determined in fitting procedure.

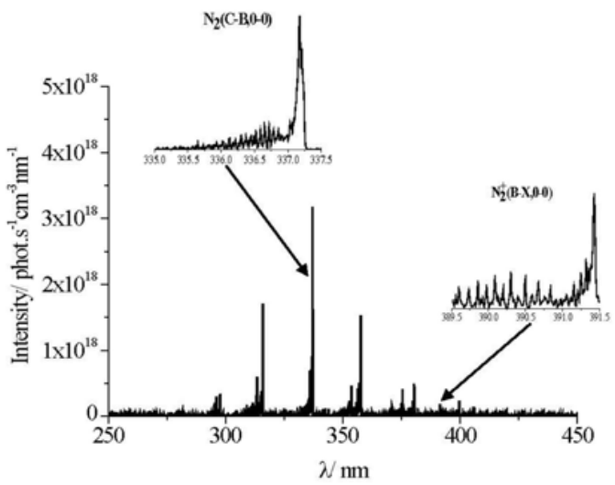

Fig. 1. Emission spectrum of DBD in air with Al-spike as opposite electrode. Inter-electrode distance amounts to 1.5 mm.

To determine real absolute intensity of photoemission in DBD, the measured emission spectrum (in counts·s^{-1} per pixel of spectrometer's CCD) is corrected to the efficiency ε (in counts·nm·photons^{-1} per pixel) of the spectrometer (Bibinov, 2007). Geometrical factor of optical diagnostics and discharge duration must also be taken into account. To determine geometrical factor for OES, two factors have to be considered namely, a) plasma volume observed by the spectrometer, and b) the fraction of photons emitted by molecules in plasma volume which reach the entrance hole of the optical fibre of the spectrometer.

To determine plasma volume which is observed by the spectrometer, acceptance angle of the optic fibre is measured. This solid angle has a cosine profile. Also, the photons emitted by excited molecules placed within this solid angle can be accepted by the optical fibre and measured by the spectrometer. For this reason, we refer to the solid angle as acceptance angle. To increase the spatial resolution of OES diagnostics, the acceptance angle of optical

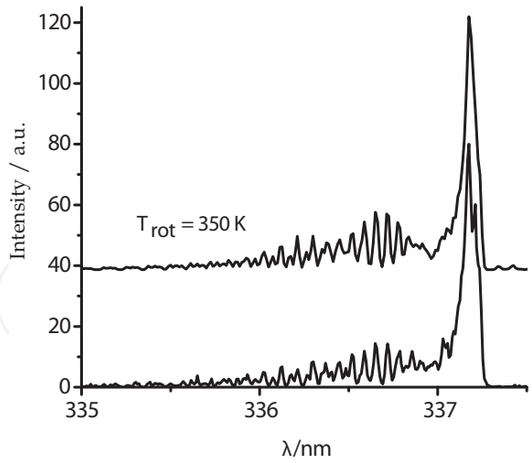

Fig. 2. Measured (bottom) and simulated (top) spectra of nitrogen emission N_2(C-B,0-0) at 1.5 mm inter-electrode distance for Al-spike. The simulated spectrum is shifted for clarity.

fibre is reduced by fitting it with a diaphragm. For OES diagnostics of DBD, an optical diaphragm with acceptance angle of ± 3° is fitted to the optical fibre. The fraction of photons emitted in acceptance angle and reaching the entrance hole of the optical fibre is calculated as the ratio between the area of entrance hole and the area of the sphere - with radius equal to the distance between the emitted molecule and entrance hole.

Generally, only Maxwell distribution function for electrons can be determined applying OES with two nitrogen bands. Maxwell distribution function is solution of Boltzmann equation (1) in assumption of ideal gas conditions, namely without taking inelastic collisions of electrons with molecules into consideration. At atmospheric-pressure conditions in DBD, inelastic collisions of electrons with nitrogen and oxygen molecules are very frequent and therefore electron distribution function differs strongly from Maxwell distribution. To solve this problem, we determine EVDF in air-DBD applying a combination of two diagnostic methods namely, numerical simulation and OES. The Boltzmann equation (1) is solved numerically in nitrogen/oxygen mixture (0.78/0.21) at atmospheric pressure, applying a program developed by the group of Prof. A P Napartovich (Stefanovich, 2001). EVDF is simulated using this program in "local" approximation by variable electric field because this parameter is not known in DBD *a priori*. "Local approximation" means that at every position EVDF can be determined from Boltzmann equation for homogeneous non-bounded plasma using local electric field strength. Therefore, EVDF in DBD is simulated applying equation (2) by neglecting the inhomogeneity term in equation (1):

$$\frac{\partial f}{\partial t} - \nabla_v \left(\frac{e}{m_e}\vec{E}f\right) = S_{coll} \tag{2}$$

Electric field strength in DBD is not known forehand. Hence, we simulate EVDF for different values of reduced electric field. Using simulated EVDF, we calculate intensities of nitrogen molecular emissions and compare them with measured ones to determine the EVDF and also the electric field strength in active plasma volume.

Intensity of molecular nitrogen emission $I_{N_2^*}$ (in photons·s^{-1}) is the integral of spectral density I_λ (in photons·nm^{-1}·s^{-1}) of measured emission spectrum and is expressed as equation (3):

$$I_{N_2^*} = \int_{\lambda} I_{\lambda} d\lambda = \int_{\lambda} \frac{I_p d\lambda}{\varepsilon(\lambda) \cdot G \cdot V \cdot F \cdot \tau} = Q_{N_2^*} \cdot [N_2] \cdot n_e \cdot k_{exc}^{N_2^*}, \quad (3)$$

where, I_p - measured emission spectrum (counts per pixel);
$\varepsilon(\lambda)$ - efficiency of spectrometer (counts·nm/photons per pixel);
G - geometrical factor
V - plasma volume observed by spectrometer (m^{-3});
F - frequency of discharge pulses (Hz); and
τ - averaged duration of discharge pulses (s).

$k_{exc}^{N_2^*} = 4\pi \cdot \sqrt{2} \int_E f_v(E) \cdot \sqrt{\frac{2 \cdot e}{m_e}} \cdot E \cdot \sigma_{exc}^{N_2^*}(E) dE$ - rate constant of excitation of nitrogen photoemission ($m^3 \cdot s^{-1}$) by electron impact.

$\sigma_{exc}^{N_2^*}(E)$ - cross section (m^2) of electron impact excitation of nitrogen photoemission (Itikawa, 2006) and
E - kinetic energy of electrons (eV).

The term $Q_{N_2^*} = \frac{A_{N_2^*}}{A_{N_2^*} + k_{N_2^*}^{N_2}[N_2] + k_{N_2^*}^{O_2}[O_2]}$ in equation (3) is the quenching factor for nitrogen emission where, $A_{N_2^*}$ - Einstein coefficient for spontaneous emission (Pancheshnyi, 2000, Kozlov, 2001);

$k_{N_2^*}^{N_2}$, $k_{N_2^*}^{O_2}$ - rate constants of quenching ($m^3 \cdot s^{-1}$) of nitrogen excited states by collisions with nitrogen and oxygen molecules, respectively (Pancheshnyi, 2000, Kozlov, 2001); and
$[N_2]$, $[O_2]$ - nitrogen and oxygen concentration (m^{-3});

Electron velocity distribution function $f_v(E)$ is normalized to fulfil equation (4):

$$4\pi \cdot \sqrt{2} \int_E f_v(E) \cdot \sqrt{E} dE = 1 \quad (4)$$

To determine discharge duration, the current through the object is measured using a current monitor. The measured current consists of the displacement current and the short discharge current pulses. Discharge duration (τ in seconds) is the full width at half maximum (FWHM) of measured discharge current pulse. To obtain the dimensions of the microdischarges, which are important for the determination of active plasma volume, microphotography using a high-speed camera with spatial resolution of 5 μm is applied.

Ratio of intensities of neutral nitrogen molecular emission N_2(C-B) to molecular ion emission N_2^+(B-X), as shown in expression (5), is used for the purpose of electric field determination.

$$\frac{I_{N_2(C-B)}}{I_{N_2^+(B-X)}} = \frac{Q_{N_2(C-B)}}{Q_{N_2^+(B-X)}} \cdot \frac{k_{exc}^{N_2(C-B)}}{k_{exc}^{N_2^+(B-X)}} \quad (5)$$

Because of difference in threshold values of electron's kinetic energy required for electron impact excitation of nitrogen emissions, and due to dependence of excitation cross section

on kinetic energy, the ratio (5) is very sensitive to variation of electric field in plasma. We solve the Boltzmann equation (2) for nitrogen/oxygen mixture at atmospheric conditions at variable electric field and determine the electron velocity distribution function for each electric field value (see fig.3). Applying these calculated electron distribution functions, we calculate excitation rate constants for nitrogen photo emissions and subsequently calculate the values of ratio (5). Calculated ratio is compared with ratio of same emissions measured using OES diagnostics. EVDF and averaged reduced electric field in observed plasma volume is determined from the best fit.
The averaged electron density is determined using measured absolute intensity of neutral nitrogen photoemission $I_{N_2(C-B)}$ in equation (6):

$$n_e = \frac{I_{N_2(C-B)}}{[N_2] \cdot Q_{N_2(C-B)} \cdot G \cdot V \cdot F \cdot \tau \cdot k_{exc}^{N_2(C-B)}} \tag{6}$$

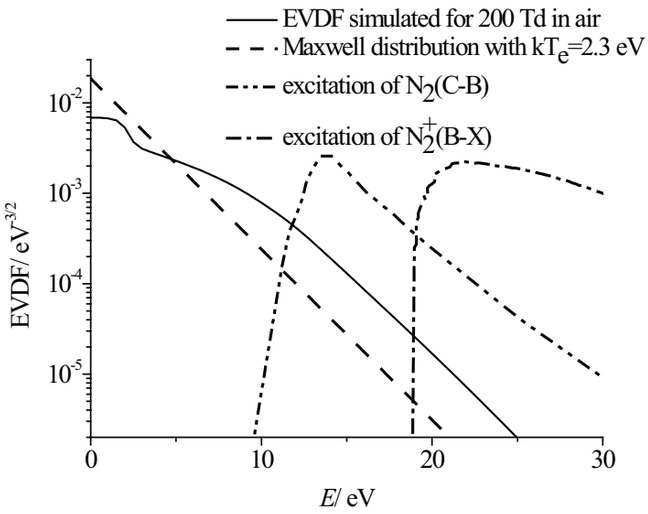

Fig. 3. Electron velocity distribution functions with the same ratio of nitrogen emissions in expression (5) simulated using numerical solution of Boltzmann equation in local approximation using equation (2) with E/N = 200 Td and Maxwell distribution function with electron temperature kT_e = 2.3 eV. Normalized integrands $f_v(E) \cdot E \cdot \sigma_{exc}^{N_2^*}(E)$ used for calculation of N_2(C-B) and N_2^+(B-X) photoemissions intensities.

5. Simulation of chemical kinetics

During discharge, chemically-active species like nitrogen and oxygen atoms and their metastables are produced by electron-impact dissociation and excitation of neutral gas molecules. Nitric oxide and ozone are produced in subsequent chemical reactions (Rajasekaran, 2009) in the discharge as well as in the afterglow phase. Chemical kinetic model of atmospheric pressure DBD in air consists of great number of reactions (Stefanovic, 2001). In the simulation presented here, we include chemical reactions (see Table 1) concerning the production and destruction of nitric oxide and ozone. Other reactions which are not included in this model have small rate constant or one (or both) of the reactants have

too small concentration in our plasma conditions. For example, in spite of the fact that O(^{1}D) metastable atoms are produced by electron impact dissociation of oxygen molecules, reactions of this metastable atom are not included in the model because of its very short life time (1.4 ns) in air at atmospheric pressure conditions, and therefore its very low concentration.

No.	Reaction	Rate constant
(7)	$O_2 + e \rightarrow O + O + e$	Calculated from EVDF, n_e
(8)	$N_2 + e \rightarrow N + N + e$	Calculated from EVDF, n_e
(9)	$N_2 + e \rightarrow N_2(A) + e$	Calculated from EVDF, n_e
(10)	$O + O + M \rightarrow O_2 + M$	$3.8{\cdot}10^{-42}\, T^{-1}\exp(-170/T)$ $m^6\, s^{-1}$
(11)	$O + O_2 + O_2 \rightarrow O_3 + O_2$	$8.6{\cdot}10^{-43}\, T^{-1.25}$ $m^6\, s^{-1}$
(12)	$N + N + M \rightarrow N_2 + M$	$8.3\cdot10^{-46}\exp(500/T)$ $m^6\, s^{-1}$
(13)	$O + O_2 + N_2 \rightarrow O_3 + N_2$	$5.6{\cdot}10^{-41}\, T^{-2}$ $m^6\, s^{-1}$
(14)	$O + O_3 \rightarrow O_2 + O_2$	$1.9{\cdot}10^{-17}\exp(-2300/T)$ $m^3\, s^{-1}$
(15)	$O + NO + M \rightarrow NO_2 + M$	$9.1{\cdot}10^{-40}\, T^{-1.6}$ $m^6\, s^{-1}$
(16)	$NO + N \rightarrow N_2 + O$	$1.8{\cdot}10^{-18}\, T^{0.5}$ $m^3\, s^{-1}$
(17)	$N + O_2 \rightarrow NO + O$	$1.1{\cdot}10^{-20}\, T\exp(-3150/T)$ $m^3\, s^{-1}$
(18)	$N + O_3 \rightarrow NO + O_2$	$5{\cdot}10^{-18}\exp(-650/T)$ $m^3\, s^{-1}$
(19)	$N + O + M \rightarrow NO + M$	$1.8{\cdot}10^{-43}\, T^{-0.5}$ $m^6\, s^{-1}$
(20)	$O_3 + NO \rightarrow NO_2 + O_2$	$9{\cdot}10^{-19}\exp(-1200/T)$ $m^3\, s^{-1}$
(21)	$N_2(A) + O_2 \rightarrow N_2 + O + O$	$1.63{\cdot}10^{-18}(T/300)^{0.55}$ $m^3\, s^{-1}$
(22)	$N_2(A) + O_2 \rightarrow N_2 + O_2$	$8.75{\cdot}10^{-19}(T/300)^{0.55}$ $m^3\, s^{-1}$
(23)	$N_2(A) + N \rightarrow N_2 + N$	$2.6{\cdot}10^{-18}\, T^{0.5}$ $m^3\, s^{-1}$
(24)	$N_2(A) + NO \rightarrow N_2 + NO(A)$	$3.5{\cdot}10^{-18}\, T^{0.5}$ $m^3\, s^{-1}$
(25)	$N_2(A) + N_2(A) \rightarrow N_2(C) + N_2$	$8.7{\cdot}10^{-18}\, T^{0.5}$ $m^3\, s^{-1}$
(26)	$O + O_3 \rightarrow O_2(a^1\Delta) + O_2$	$6.3{\cdot}10^{-18}\exp(-2300/T)$ $m^3\, s^{-1}$
(27)	$O + O_3 \rightarrow O_2(b^1\Sigma) + O_2$	$3.2{\cdot}10^{-18}\exp(-2300/T)$ $m^3\, s^{-1}$

Table 1. Plasma-chemical reactions and their rate constants (Stefanovich, 2001) included in the simulation.

The temporal behavior of chemically-active species produced in the discharge, and the fluxes of nitric oxide and ozone to the surface of the treated electrode both in the homogeneous and stochastically-distributed discharges are simulated. The equations, the boundary conditions and the assumptions made for this simulation are discussed briefly in the following sections.

5.1 Equation

The temporal behavior of the chemically-active species produced in the discharge is described by the equation of continuity (28). Gain and loss of the active species by different reactions in the discharge channel and their diffusion (according to Fick's law) are considered.

$$\frac{\partial[M]}{\partial t} = \nabla \cdot (D(T)\nabla[M]) + \sum k_{MN}(T)[M][N], \tag{28}$$

where $[M]$ and $[N]$ (in m^{-3}) are the densities of species involved in the chemical reaction, $D(T)$ (in $m^2 \cdot s^{-1}$) is the diffusion coefficient, and k_{MN} (in $m^3 \cdot s^{-1}$) is the rate constant of the corresponding chemical reaction. It describes the temporal evolution of species' density due to diffusion (first term on the right hand side of equation (28)) and different chemical reactions (second term). Cylindrical symmetry of the discharge is assumed and dependencies along the azimuth co-ordinate are neglected. Since plasma heats up the gas and the rate constants of the chemical reactions are temperature dependent, the equation of thermo-conductivity (29) is solved in the afterglow phase.

$$\frac{\partial T}{\partial t} = \nabla \cdot (\Lambda(T_g)\nabla T_g), \tag{29}$$

where T_g (in K) is the gas temperature and $\Lambda(T_g)$ (in $m^2 \cdot s^{-1}$) is the thermal diffusivity. $\Lambda(T_g)$ and $D(T_g)$ are interpolated, respectively, in equations (30) and (31) (Kohlrausch, 1996 & Marrero, 1972).

$$\Lambda(T_g) = 1.19 \cdot 10^{-6} T_g^{\,2} + 7.76 \cdot 10^{-4} T_g - 0.1 \tag{30}$$

$$D(T_g) = D_0 (T_g / 273)^{\beta}, \tag{31}$$

where D_0 is the diffusion constant with a value of $0.28 \cdot 10^{-4}$ $m^2 \cdot s^{-1}$ for oxygen atoms, $0.29 \cdot 10^{-4}$ $m^2 \cdot s^{-1}$ for nitrogen atoms, $0.182 \cdot 10^{-4}$ $m^2 \cdot s^{-1}$ for nitrogen metastables and nitric oxide, and $0.170 \cdot 10^{-4}$ $m^2 \cdot s^{-1}$ for ozone (Eliasson, 1987). The parameter β in equation (31) is 1.774 for diffusion of oxygen and nitrogen atoms, 1.724 for nitrogen molecules and nitric oxide, and 1.750 for ozone.

5.2 Assumptions for homogeneous discharge mode

In the homogeneous discharge mode, the plasma appearing between the electrodes is approximately in cylindrical volume, since the upper electrode is circular in shape and is separated by a small gap from the opposite electrode. In such a discharge, the chemically-active species produced in the plasma can diffuse out of this cylindrical volume. The simulation is halted when a periodical behavior for all calculated values reaches saturation.

The flux of active species $\Gamma_{z,hom.}(r)$ (in $m^{-2}\cdot s^{-1}$) to the surface of treated electrode is then calculated in the final step by averaging the flux $\Gamma_z(r,t)$ (in $m^{-2}\cdot s^{-1}$) in equation (32) over time as shown in (33):

$$\Gamma_z(\mathrm{r,t}) = -D\frac{\partial[M](\mathrm{r,t})}{\partial z} \tag{32}$$

$$\Gamma_{\mathrm{z,hom.}}(\mathrm{r}) = \frac{1}{\mathrm{t_{pulse}}}\int_0^{\mathrm{t_{pulse}}} \Gamma_z(\mathrm{r,t})\ \mathrm{dt}, \tag{33}$$

where t_{pulse} is the reciprocal frequency of applied high voltage.

5.3 Assumptions for filamentary discharge

Filamentary discharge is ignited in cylindrical channel with length equal to the inter-electrode distance. Gas temperature and plasma parameters are assumed constant in the whole plasma volume during all discharge pulse. Surrounding gas temperature amounts to 293 K.

6. Results

6.1 DBD plasma source

The DBD plasma source for biomedical applications consists of a ring-shaped upper (copper) electrode (diameter = 8 mm) which is covered with a thin layer of ceramic (Al_2O_3) for a thickness of 1 mm. In principle, the human body, which has high capacitance, can be used as the opposite electrode (fig.4). Discharge is ignited when the distance to the finger surface is lower than about 2 mm. Dependence of ignition conditions on treated substrate (skin or nail) and on surface conditions (wet or dry surface) is not yet clear. The voltage amplitude and pulse frequency of power supply are selected in such a way that there is no pain caused during DBD treatment of human body.

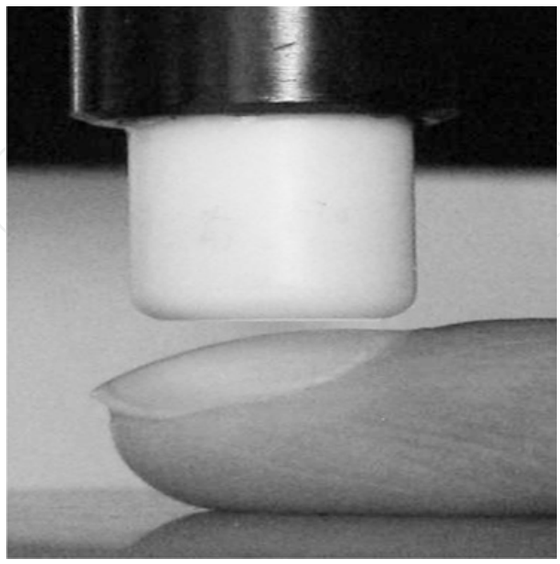

Fig. 4. Snapshot of DBD plasma source for treatment of biological objects

6.2 Microphotography

Dielectric barrier discharge is ignited in air between the upper electrode and the opposite electrode which is grounded or with a high-capacitance material like human body. According to our observations, the DBD source operated directly on human body (on the inner side of the fore finger) ignites a "twin discharge" which shows both homogeneous and filamentary regimes (Fig.5A). DBD ignited on the mouse skin surface consists also of homogeneous and filamentary discharges (see fig. 5B). The latter ignite on the some raised points (obviously hairs) for each trigger pulse. We call such a discharge as 'single-filamentary discharge' to distinguish it from normal filamentary discharge in DBD ignited on conductive electrode and which consists of number of stochastically distributed discharge channels.

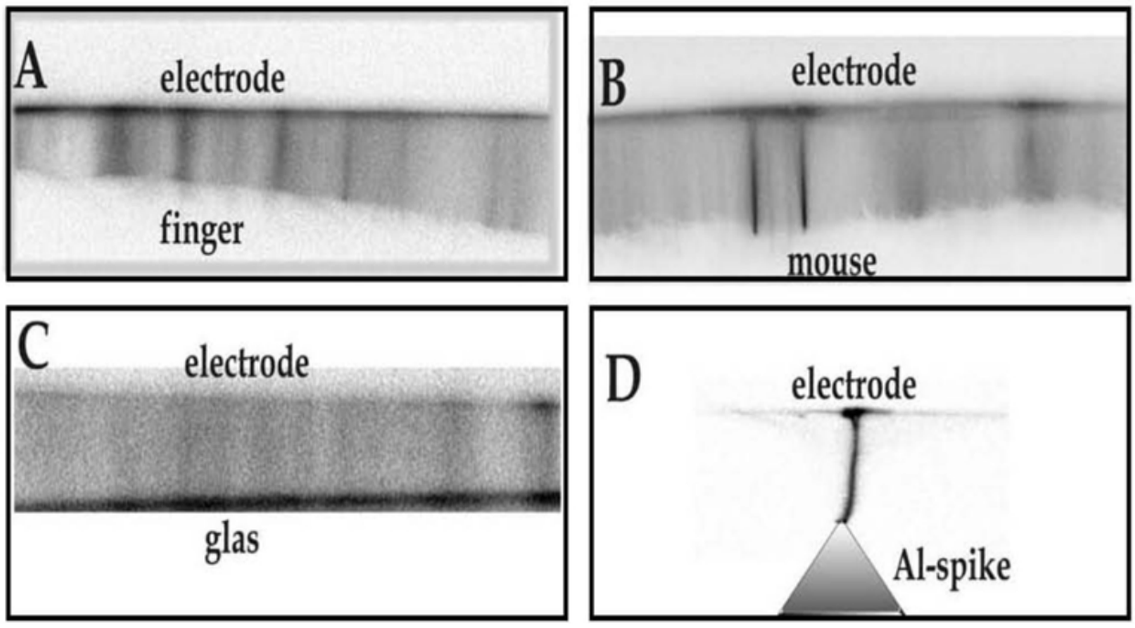

Fig. 5. Microphotography (negative image) of simultaneous homogeneous and filamentary discharges on inner side of finger (A), mouse skin (B), homogeneous discharge on glass (C) and single-filamentary discharge on Al-spike (D). Exposure time of microphotography is lower than the period of high voltage pulses.

To study and optimize the DBD source for biomedical application, especially for therapeutic use, characterization and study of factors influencing the formation of this "twin discharge" are required. Characterization of the discharge on the body of different individuals will yield results with large degrees of freedom. The varied results could be due to the different skin properties between individuals and within the same individual also. Optimization of the DBD source based on such studies are necessary at the later stages. Before that, the different discharge modes in air and the causes for such modes require detailed investigation. For this purpose, we characterize DBD operated individually in homogeneous and filamentary modes using electrodes of different materials and profiles. We observed a homogeneous discharge (figure 5C) when glass is used as the opposite electrode, and a single-filamentary discharge is ignited with aluminium spike (figure 5D). We characterize these modes individually to learn the differences in plasma conditions between the modes

and to understand the influence of the opposite electrode (its material and profile) on discharge formation. The diameter of the single-filamentary microdischarges on mouse skin and on Al-spike is comparable and amounts to about 50 μm.

6.3 Voltage-current characteristics

The voltage at the upper electrode is measured using a capacitive voltage divider (dividing factor of 1: 2000) and plasma current is measured using a current monitor (Pearson - 2877 with 1V:1A output). Voltage and current traces are recorded using an oscilloscope. A high voltage pulsed power supply of 300 Hz frequency and amplitude up to 14 kV is used (figure 6a). Each high voltage pulse has a sequential profile with damped oscillations and frequency of about 100 kHz (figure 6b). Micro discharges are ignited if the breakdown conditions in the gas gap are fulfilled. These breakdowns occur in the first quarter of the power supply period (figure 7a). The next discharge ignites at lower applied voltage because of the charged dielectric surface and, therefore, high electric field in the gas gap after first discharge. Second (and following) ignition can occur even at 0 V.

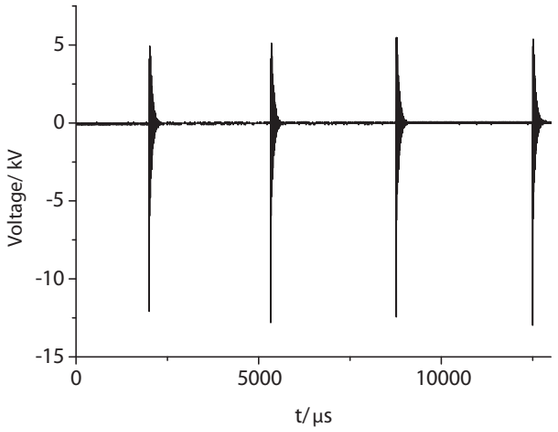

Fig. 6a. Profile of high voltage pulses

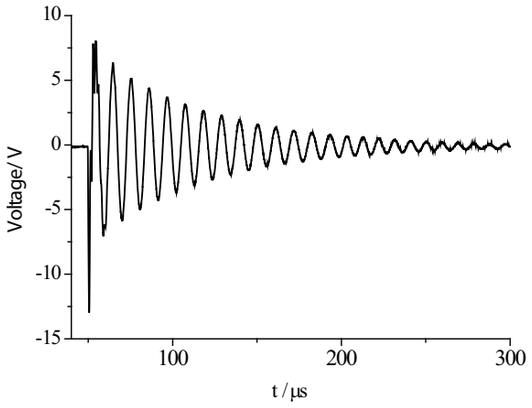

Fig. 6b. Sequence of high voltage pulses initialized by one trigger pulse

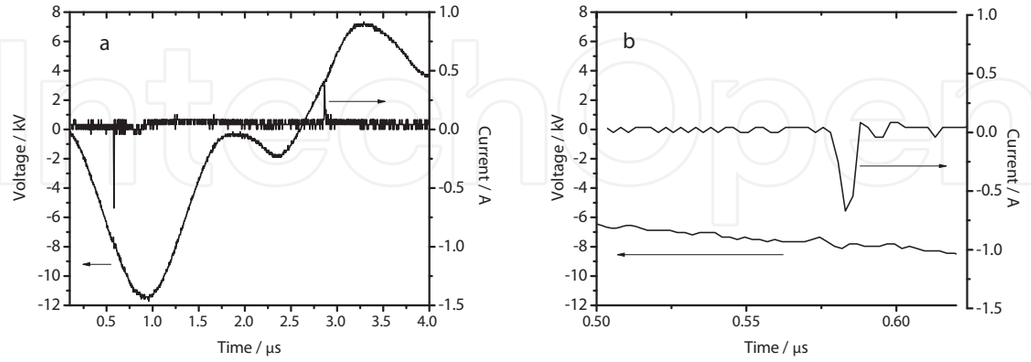

Fig. 7. Current-voltage characteristics for glass opposite electrode at 1 mm inter-electrode distance with different time resolution

To determine discharge duration (τ (in ns)), we measure the full width at half-maximum (FWHM) from the profile of the current pulses (figure 7b). These values for different DBD conditions and number of ignitions for each trigger pulse are presented in Table 2.

Opposite electrode / Parameters	Mouse (d = 1 mm)	Mouse (d = 0.5 mm)	Glass (d = 1 mm)	Al-spike (d = 1.5 mm)
τ (ns)	25 ± 5	25 ± 5	6.0 ± 1.5	23 ± 1
No. of ignitions	3	5	2	1

Table 2. Pulse duration (at FWHM) and number of discharge pulses per trigger pulse in DBD with different opposite electrodes

6.4 Gas temperature

The gas temperature in the active plasma volume, determined for DBD treatment of mouse skin, is 320 ± 20 K for both 1 mm and 0.5 mm gaps (table 3). It is worth mentioning here that the same temperature is obtained for the homogeneous discharge with glass as the opposite electrode. The gas temperature in discharge with Al-spike (T_g = 350 K) is higher than the surrounding gas temperature (T_g = 293 K) but decays back to surrounding gas temperature in afterglow phase. Solving thermo-conductivity equation (27), we calculate the spatial temperature profiles at different delay times in afterglow of micro discharges. In this calculation, we use 50 μm for diameter of discharge channel, a surrounding gas temperature of 293 K, and 350 K gas temperature in discharge channel. In afterglow phase, the gas temperature decreases rapidly (figure 8).

Opposite electrode	Mouse (d = 1 mm)	Mouse (d = 0.5 mm)	Glass (d = 1 mm)	Al-spike (d = 1.5 mm)
T_g (K)	320 ± 20	320 ± 20	320 ± 20	350 ± 20

Table 3. Gas temperature determined in DBD with different opposite electrodes

For simulation of chemical kinetics in active and afterglow phases of DBD on mouse skin, we assume that gas temperature as 310 K because the normal body temperature of the mouse is about 315 K and the ceramic that covers the electrode has a temperature of about 300 K during experiment. During active phase of the discharge, the gas temperature increases up to about 320 K, but in short time it decays to the steady state value of about 310 K.

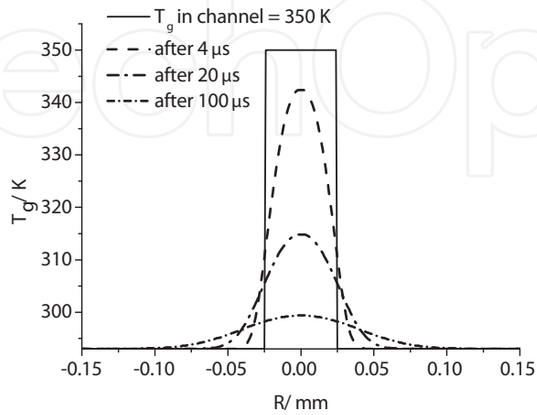

Fig. 8. Spatial distribution of the gas temperature (radially along the electrode) in the afterglow phase in the gap between electrodes for Al-spike as the opposite electrode.

6.5 Plasma parameters

Microphotography of discharge on the mouse skin shows homogeneous and single-filamentary discharges ignited simultaneously. Because of low emission intensity of single-filamentary discharge (accounting for only about 6 % of the total observed emission) in relation to the homogeneous discharge, plasma parameters are determined for the homogeneous discharge. However, the influence of single-filamentary discharge on total fluxes of chemically-active species by DBD treatment of biological object is qualitatively discussed in section 6.7.

The plasma parameters (reduced electric field and electron density) determined in DBD at different plasma conditions and dissociation cross sections of nitrogen and oxygen molecules calculated applying these plasma parameters and equation (34) are presented in table 4.

$$k_{diss} = 4\pi \cdot \sqrt{2} \int_E f_v(E) \cdot \sqrt{\frac{2 \cdot e}{m_e}} \cdot E \cdot \sigma_{diss}(E) dE, \tag{34}$$

where $\sigma_{diss}(E)$ - dissociation rate constants of nitrogen (Itikawa, 2006) and oxygen molecules (Itikawa, 1989). Reduced electric field E/N is expressed in Townsend (Td) where N is the gas density (1 Td = 10^{-21} V·m^2). E/N for different electrodes are listed in table 4.

E/N in homogenous discharge on mouse skin increases with decrease of the inter-electrode distance but is lower than that in single-filamentary mode and in homogeneous discharge on glass.

Opposite electrode	**d mm**	**E/N Td**	**n_e m^{-3}**	**k_{diss} N_2 10^{-15} m^3·s^{-1}**	**k_{diss} O_2 10^{-15} m^3·s^{-1}**
Mouse skin	0.5	290	$7.3 \cdot 10^{16}$	2.5	0.77
	1	280	$7.1 \cdot 10^{16}$	2.4	0.74
Al-spike	0.5	430	$4.2 \cdot 10^{21}$	4.4	1.16
	1	406	$2.4 \cdot 10^{21}$	3.9	1.11
Glass	0.5	360	$4.3 \cdot 10^{17}$	4.1	1.13
	1	320	$3.7 \cdot 10^{17}$	3.2	1.03

Table 4. Reduced electric field (E/N), electron density (n_e) for DBD on mouse skin, Al-spike and glass at different inter-electrode distances (d), and the rate constants for electron-impact dissociation of nitrogen (k_{diss} N_2) and of oxygen (k_{diss} O_2) molecules calculated using equation (34).

Electron densities in active plasma volume measured applying neutral nitrogen molecular emission by variable plasma conditions are presented in table 4. The electron density in homogeneous mode of DBD is lower than that in filamentary mode.

Using determined electric field, the electron velocity distribution functions in DBD are simulated (fig.9).

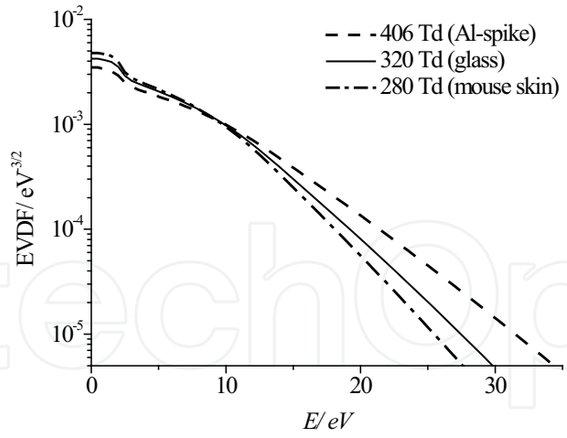

Fig. 9. Electron velocity distribution functions determined using OES and numerical simulation in DBD in air at atmospheric pressure with 1 mm inter-electrode distance and different opposite electrodes.

6.6 Validation test of 'plasma characterization with low spatial resolution OES diagnostics'

The plasma parameters (electron density and reduced electric field) are determined in this work using simulation and two spectral bands namely, the excitation emission of N_2(C-B) and of N_2^+ (B-X). These plasma parameters are averaged values in the volume observed by the spectrometer. From microphotography, it is clear that in this experiment two discharge conditions exist: i) a homogeneous discharge in the gap between the electrodes, and ii) the occurrence of microdischarge filaments along with this homogeneous discharge. Electric field and electron density differ strongly in these two DBD modes (see table 4). Furthermore, plasma parameters in homogeneous and in filamentary discharges have fine structures with higher variations of electric field and electron density with distance from the electrodes (Braun, 1992; ; Massines 1998 & Kozlov, 2001).

We study the influence of low spatial resolution of OES diagnostics on determined plasma parameters through simulation of plasma conditions with variable spatial resolution. We assume that our spectrometer observes two plasma volumes with very different electric field, one with 100 Td and the other with 1000 Td. n_e for 100 Td is assumed as $7 \cdot 10^{16}$ m^{-3} (same as that determined for 1 mm in discharge on mouse skin). Using these assumptions, we perform the validation for two cases:

i. ***First case -*** it is assumed that the two plasma volumes produce equal intensities of neutral nitrogen emission ($I_{N_2(C-B)}$). n_e at 1000 Td is calculated to be $1.4 \cdot 10^{15}$ m^{-3}. Also, the total N_2(C-B) emission intensity is the sum of $I_{N2(C-B)}$ from the two plasma volumes. 'Averaged' *E/N* is estimated from the ratio of total N_2(C-B) emission intensity to the total N_2^+ (B-X) emission intensity. Accordingly, 'averaged' *E/N* = 610 Td and corresponding n_e is calculated as $1.7 \cdot 10^{15}$ m^{-3}.

ii. ***Second case -*** it is assumed that the two plasma volumes produce equal intensities of nitrogen-ion emission ($I_{N_2^+(B-X)}$). n_e at 1000 Td in this case is $1.5 \cdot 10^{12}$ m^{-3}. The total emission intensity of N_2^+ (B-X) is calculated as the sum of $I_{N_2^+(B-X)}$ from the two plasma volumes. 'Averaged' *E/N* = 110 Td estimated in the same way as in the *first case*. n_e for 110 Td is $2.8 \cdot 10^{16}$ m^{-3}.

It can be seen that the 'averaged' plasma parameters differ strongly from space-resolved plasma parameters. But the main aim of plasma characterization is the determination of dissociation rates of nitrogen and oxygen molecules (processes (7) and (8) in table 1). These values are subsequently used in the simulation of chemical kinetics in active plasma volume and in afterglow. We calculate the dissociation rates of diatomic molecules using space-resolved parameters and compare them with the corresponding dissociation rates calculated using 'averaged' plasma parameters.

The dissociation rate constant of nitrogen molecules ($k_{diss}^{N_2}$) and of oxygen molecules ($k_{diss}^{O_2}$) using 'averaged' parameters and using the space-resolved parameters are calculated. The ratio of $k_{diss}^{O_2}$ at 'averaged' condition to that at the space-resolved condition is determined as 1.03 for the *first case* and 1.2 for the *second* case. Similarly, the ratio of $k_{diss}^{O_2}$ in the 'averaged' conditions to that in the space-resolved condition corresponds to 0.47 for the *first case* and 1.2 for the *second* case. All the values are presented in table 5.

Plasma conditions assumed for validation of averaged plasma parameters	$\frac{k_{diss}^{N_2}\text{averaged conditions}}{k_{diss}^{N_2}\text{spatial-resolved conditions}}$	$\frac{k_{diss}^{O_2}\text{ averaged conditions}}{k_{diss}^{O_2}\text{spatial-resolved conditions}}$
First case $I_{N_2(C\text{-}B)}$ at 100 Td = $I_{N_2(C\text{-}B)}$ 1000 Td at 100 Td, $n_e = 7 \cdot 10^{16}$ m^{-3} at 1000 Td, $n_e = 1.4 \cdot 10^{15}$ m^{-3} 'averaged' E/N = 610 Td; $n_e = 1.7 \cdot 10^{15}$ m^{-3}	1.03	0.47
Second case $I_{N_2^+(B\text{-}X)}$ at 100 Td = $I_{N_2^+(B\text{-}X)}$ 1000 Td at 100 Td, $n_e = 7 \cdot 10^{16}$ m^{-3} at 1000 Td, $n_e = 1.5 \cdot 10^{12}$ m^{-3} 'averaged' E/N = 110 Td; $n_e = 2.8 \cdot 10^{16}$ m^{-3}	1.2	1.2

Table 5. Plasma conditions assumed for validation of averaged plasma parameters and the corresponding dissociation rate constants for nitrogen ($k_{diss}^{N_2}$) and oxygen ($k_{diss}^{O_2}$).

When the neutral nitrogen emission in the region of high electric field is *weaker* than that in the region of low electric field (due to small number of electrons resulting from either low electron density or small plasma volume), then the averaged E/N calculated (110 Td) is closer to the E/N value of the low electric field (i.e. 100 Td) as seen in the *second case* of this estimation. In such a condition, the dissociation rates of oxygen and nitrogen molecules calculated using 'averaged' plasma parameters differ only slightly from the values determined with space-resolved plasma parameters.

Conversely, if neutral nitrogen emission in the region of high electric field is *equal* or *comparable* to that in the low electric field region, then the 'averaged' E/N calculated (610 Td) is closer to the E/N value of the high electric field (i.e. 1000 Td) as seen in the *first case* of this estimation. In this case, as can be seen in the table 5, the dissociation rate of oxygen

calculated using 'averaged' plasma parameters is under-estimated by a factor of about 2. At the same time the dissociation rate of nitrogen calculated using 'averaged' parameters did not show large deviations from the corresponding value calculated at space-resolved condition. The reason for this effect is the difference between threshold values of dissociation cross-section of nitrogen and oxygen molecules, and the difference of the 'averaged' electron distribution function from the space-resolved one. To determine dissociation rates with better accuracy at such plasma conditions space and time resolved optical emission diagnostic is needed.

When the same validation procedure was performed for two plasma volumes with 200 Td and 1000 Td, the dissociation rate of oxygen and nitrogen molecules calculated using 'averaged' parameters varied only slightly (less than 20 %) from that calculated using space-resolved parameters in the *first case* as well as in the *second case*. Hence, it can be concluded that our estimation method holds good for calculation of 'averaged' *E/N* when the plasma volumes are assigned with *E/N*=200 Td or higher. The previous condition where 100 Td and 1000 Td were assumed for estimation proves to be a severe case for this estimation procedure.

Because of relatively low averaged electric field (*E/N* ~ 300 - 400 Td) determined in DBD at plasma conditions considered here, we can establish that the influence of regions with high electric field is not so strong (as seen in the *first* case considered above). The difference in the calculated dissociation rates of nitrogen and oxygen is lower than a factor of 2 according to this estimation but actual values in the experiment will be determined in forthcoming work through space-resolved diagnostic methods.

Nevertheless, the rate of dissociation of diatomic molecules in active plasma volume is reliable (with possible deviation lower than factor 2) despite the difference between the averaged plasma parameters (determined for DBD in air at atmospheric pressure using OES) and the actual plasma parameters existing in the studied DBD conditions.

6.7 Fluxes of ozone and nitric oxide (NO)

The fluxes of ozone and NO reaching the treated surface in our plasma conditions are shown in figures 10(a) and 10(b), respectively. As it can be seen from these figures, the flux of ozone and NO determined for the homogeneous discharge on the mouse skin is similar to that for the homogeneous discharge with glass. Despite lower electric field and electron density, the fluxes of ozone and nitric oxide on the mouse skin are similar to the fluxes on glass surface which is due to the longer pulse duration and increased number of current pulses in the former.

Though the discharge ignited on mouse is assumed to be homogeneous, the influence of the simultaneously-occurring filamentary discharges (figure 5B) on the chemical kinetics cannot be ignored and is only qualitatively discussed here. From the fluxes of NO and ozone simulated for a single-filamentary discharge, it is observed that these fluxes are the highest when compared to the other modes (Rajasekaran, 2009 & Rajasekaran, 2010). However, it should be noted that the NO and ozone fluxes for a single-filamentary discharge is comparable to the respective flux in the other discharges for a small region close to the vertical axis along the length of the filament as seen in figures 10(a) and 10(b).

To compare the applications of our DBD with other plasma sources for e.g. with 'indirect' plasma sources where the relative proportion of ozone and nitric oxide in its effluent is known, we estimate the flux $\frac{[M]\cdot v_{mean}}{4\cdot 10^6}$ of chemically-active species in the DBD source

with the assumption that steady state concentration of chemically-active species in air is 1 ppm (one part per million) (figure 10). For this estimation, the mean velocity (v_{mean} in m·s^{-1}) and density of nitrogen and oxygen molecules ([M] in m^{-3}) are about 460 m·s^{-1} and 2.5·10^{25} m^{-3} correspondingly at 293 K.

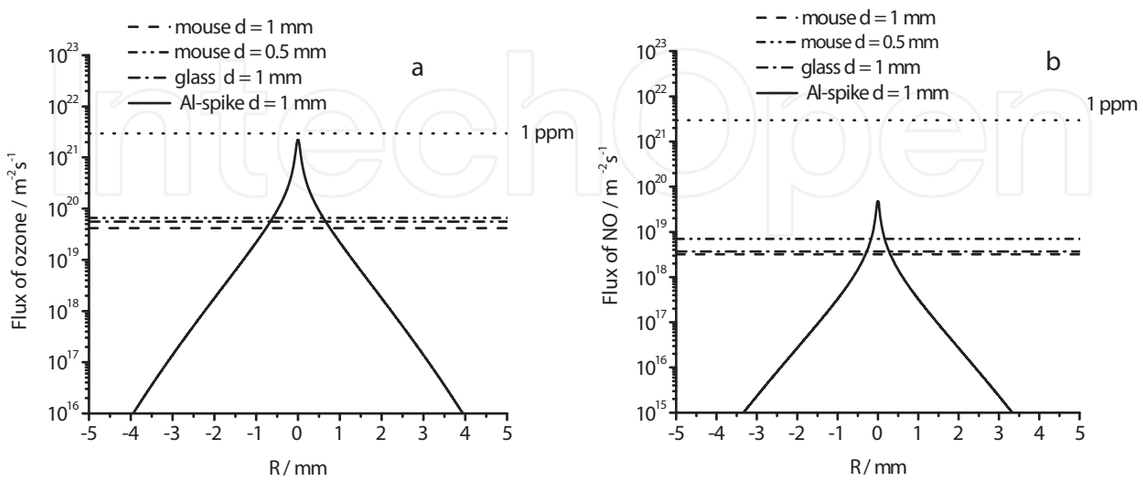

Fig. 10. Flux of ozone (a) and nitric oxide (b) reaching the treated surface across the radius of the driving electrode (R) for DBD on different substrates. The fluxes at species' concentration of 1 ppm are calculated using mean velocity and concentration of nitrogen and oxygen molecules at plasma conditions.

6.8 UV-irradiation

The UV-irradiation of mouse skin is 210 mW·m^{-2} for 0.5 mm gap, and 252 mW·m^{-2} for 1 mm gap. By decrease of inter-electrode distance, plasma volume decreases but at the same time electric field and electron density and, therefore, excitation rate constants for nitrogen UV-emission increase (see figure 11). Intensity of NO-emission in UV-C region (λ < 280 nm) is detected only for single-filamentary discharge with Al-spike and irradiation reaches a maximum of about 10 mW·m^{-2} near the discharge channel. UV-C emission for homogenous discharges on the mouse skin and glass is not detectable. We can only estimate that UV-C irradiation in this DBD mode is lower than 2 mW·m^{-2}. The irradiation of UV-A and UV-B in the UV-A - UV-B therapy used for treating atopic dermatitis (Jekler,1990) is presented in figure 11.

7. Discussion

Concentrations and fluxes of nitric oxide and ozone during DBD treatment are complicated functions consisting of parameters pertaining to different plasma conditions. The nitrogen and oxygen atoms are generated during electron impact dissociation and are lost in gas phase recombination process for the production of nitrogen and oxygen molecules. At atmospheric pressure conditions, nitric oxide and ozone molecules are also produced in the recombination process in gas phase. The loss of nitric oxide and ozone molecules occurs mainly during reactions with nitrogen atoms. These molecules produced both in the discharge and in the afterglow phase reach the surface of opposite electrode by diffusion.

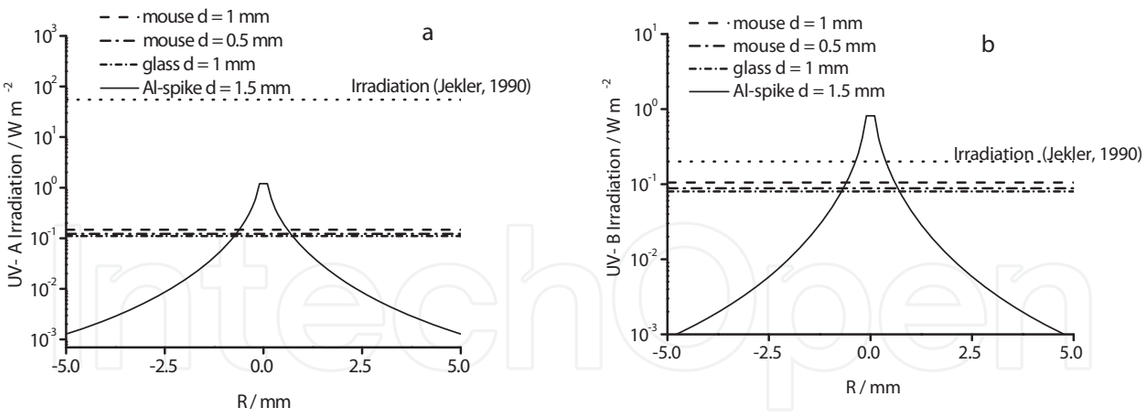

Fig. 11. Simulated UV-A (a) and UV-B (b) irradiation of treated surface for different electrode and irradiation accordingly to (Jekler, 1990).

According to our simulation, the fluxes of ozone (figure 10a) and nitric oxide (figure 10b) to the treated surface by applying our DBD in homogeneous mode is about an order of magnitude higher than that in stochastic filamentary DBD ignited on conductive Al-plate and PBS (phosphate buffered saline) solution (Rajasekaran, 2010). In both cases, the area of treated surface is approximately equal to the surface of the driving electrode. Moreover, the fluxes of nitric oxide and ozone obtained when the DBD is operated in the single-filamentary mode is higher (also about an order of magnitude) in the small area near the position of the filament. Therefore, it can be concluded that, when using the DBD plasma source for medical applications, homogeneous mode is more effective for treatment of large substrate area and single-filamentary mode is suitable for local treatment.

Both filamentary and homogeneous modes of DBD are useful for bio-medical applications like NO-therapy and ozone-therapy of skin diseases. Nitric oxide is also synthesized by skin cells during the wound healing process. This molecule plays important biological functions in the human skin as a "signaling" molecule and mediates cellular activities not only during the proliferative phase but also throughout the wound healing process (Bruch-Gerhurz, 1998, Cals-Grierson, 2004 & Childress, 2002). The low nitric oxide flux could be useful for assisting the skin cells during the different phases of wound-healing.

Ozone is a recognized 'remover' of bacteria, fungi and viruses and is used as an additional medical treatment in dermatology, stomatology, etc. Over-exposure to ozone can harm the lungs and cause irritation in the respiratory system. Therefore, the production and use of ozone are regulated by strict exposure limits, and therapeutic doses are usually higher than this permissible limit. This complexity can be overcome using DBDs generating ozone close to the treated surface. In this way, DBDs are advantageous when compared with other plasma sources which produce ozone in some active plasma volume that has to be then transported to the surface for treatment. By applying DBD in single-filamentary mode, concentration of ozone can reach 1 ppm and even more at some treatment point (Figure 10). However, ozone concentration at the distance of even 1 mm away from this point amounts to lower orders of magnitude and hence can be used for therapies which also complies with the safety norms.

7.1 Filamentary and homogeneous modes of DBD

DBD in air can be operated in both modes namely filamentary and homogeneous. Irradiation of the treated surface by photons and chemically-active species is about an order

of magnitude higher in the homogeneous DBD (Rajasekaran, 2010) when compared to the filamentary DBD. Therefore, conditions for transformation of DBD modes are very important for treatment optimization.

Previously, several investigators have used glass as dielectric for study of DBD in air at atmospheric pressure and have presented different results. Kozlov *et al* (Kozlov, 2001) reported the development of microdischarge (MD) channels in the "two-sided" barrier discharge (BD) using a pair of glass-covered electrodes powered by 6 kHz AC power supply, whereas homogeneous DBD discharges operated at nanosecond-pulsed power supply have also been reported (Walsh, 2008 & Ayan, 2009). Frequency of high-voltage pulses in sequence applied to our DBD source is about 100 kHz, yet we obtain a homogeneous discharge with glass which acts as a dielectric barrier when placed on the grounded aluminium base. This regime of homogeneous discharge could be the intermittent discharge which falls in between the above mentioned discharges (Kozlov, 2001 & Ayan, 2009).

In all cases, the primary element of each breakdown is an individual avalanche that propagates to the anode. When the avalanche moves forward, the total number of electrons increases exponentially ($e^{(\alpha-a)x}$, where α is Townsend's first coefficient, and a is attachment coefficient). The space charge generated in the avalanche generates its own electric field that distorts it. The space charge field also increases the electric field in front of the avalanche's head. This additional field is proportional to the electron number in the head of the avalanche and increases along the traversed path. When electric field in front of the avalanche head reaches a critical value, the avalanche transforms in to a streamer. In this case, the space charge grows additionally due to secondary avalanches propagating in the high electric field region and the anode-directed streamer is produced. If the distance between the electrodes is smaller than 50 mm, primary avalanches in air at atmospheric pressure cannot transform into anode-directed streamer (Raizer, 1997).

In our plasma conditions, breakdown occurs according to Townsend mechanism and the primary avalanches reach the surface of the anode. This model is confirmed in our microphotography of DBD with glass as opposite electrode. The intensity of photo emission is proportional to the electron density and hence has maximum emission near the surface of the glass, i.e. near the anode (figure 5C). After primary avalanches reach the anode, two different discharges can be ignited, either a filamentary discharge or homogeneous discharge. In the filamentary discharge, cathode-directed streamer starts in the tail of primary avalanche. Because of low mobility of heavy ions, the tail of avalanche has abundant positive charges. If the head of avalanche touches the conductive anode (e.g. aluminium plate), then the electrons are lost from the air gap, and the positively-charged avalanche trace rapidly increases electric field that can reach critical value for streamer initiation. If the anode is non-conductive (e.g. glass), electrons are *not* lost from the air gap and negative charge on the surface of the glass compensate, particularly, the positive charge of the avalanche trace. Therefore, conductivity of the anode can influence the transformation of Townsend discharge in to filamentary or homogeneous discharge.

During propagation of the avalanches, a number of metastable molecules are excited in the air gap. Energy-pooling ionization reactions like (35, 36)

$$N_2(a'^1\Sigma_g^-) + N_2(A^3\Sigma_u^+) \rightarrow N_2^+ + N_2(X) + e \quad (35)$$

$$N_2(a'^1\Sigma_g^-) + N_2(a'^1\Sigma_g^-) \rightarrow N_2^+ + N_2(X) + e, \quad (36)$$

can give rise to "seed electrons" and these electrons can initiate new avalanches. Because of relatively lower density of metastables excited in primary avalanches, energy-pooling ionization in the tail of the avalanches is delayed. These electrons are not lost from the air gap immediately after the avalanche contacts with the anode surface; instead they compensate the positive charges, particularly those in the avalanche trace. As a result, there are difficulties arising for the production of the cathode-directed streamer. The electric field in this region, for the initiation of secondary avalanches by the seed electrons, is reduced by the electric field of polarized charges of the avalanche. This causes a drop in electron number produced in the secondary avalanches. In addition, the drop in electron number is also because of the sensitivity of ionization coefficient α to the electric field variation. Hence, increase of external electric field can increase metastable excitation and thereby increase the number of seed electrons, thus preventing streamer production due to charge compensation as discussed above. The shorter rise time of the external voltage in our experiment (since the high-voltage pulses has 100 kHz frequency) could be the reason of homogeneous discharge ignition with glass as opposite electrode whereas at similar conditions but at lower frequency (6 kHz), a filamentary discharge is ignited (Kozlov, 2001). The profile of the high voltage pulse and the current-voltage characteristics for glass at an inter-electrode distance of 1 mm are shown, respectively, in figure 6 and figure 7.

7.2 Comparison of irradiation of treated surface with other treatment methods

The studied DBD source produces fluxes of photons on the treated object's surface. This flux can be compared with that of known light sources used for bio-medical applications. Phototherapy using ultraviolet radiation is available for treatment of numerous skin disorders.

The irradiation of the treated surface by UV-A and UV-B in different discharge modes are shown in figure 11a and 11b respectively. Ultraviolet A (UV-A, 320 – 400 nm) and ultraviolet B (UV-B, 280 – 320 nm) are selectively used for treatment of skin diseases like psoriasis (Coven, 1997), atopic dermatitis (Krutmann, 1992), localized scleroderma (Stege, 1997) and vitiligo (Kumar, 2009). UVA-UVB therapy is more efficient than UV-B therapy for treating skin diseases like atopic dermatitis (Hannuksela, 1985 & Jekler, 1990). Accordingly, emission from this DBD source in the wavelength range of 310 – 340 nm with a peak at 320 – 330 nm can be used for treatment of atopic dermatitis. The irradiation of UV-A and UV-B in the UVA-UVB therapy (Jekler, 1990) is comparable with that of our DBD source operated in single-filamentary mode in a region of about 1 mm diameter of the upper electrode (figure 11). Furthermore, single-filamentary DBD emits photons in the UV-C range. This irradiation can be compared with UV-C irradiation in the range of 200 – 280 nm produced in an inductively coupled plasma (ICP) reactor and applied to deactivate spores of *Bacillus atrophaeus* (Halfmann, 2007). These bacteria are commonly used as "challenging organisms" for sterilization-validation studies. UV-C irradiation near the plasma channel in single-filamentary mode of our DBD source, for a treatment time of about 10 minutes, is comparable with the ICP reactor which causes sterilization in 60 seconds with a logarithmic reduction of about 5.

Irradiation by homogeneous discharge is higher compared to that of stochastic filamentary discharges (Rajasekaran, 2010). By increasing the treatment time by two to three orders of magnitude, irradiation similar to that reported by (Jekler, 1990) can be achieved with our DBD plasma source. As in the case of UV-B for skin treatment, the irradiation values for the DBD plasma source operated in different discharge modes also appears to be comparable to

that used in the treatment of atopic dermatitis (Jekler, 1990). Through such comparisons, it is possible to optimize the plasma source in terms of treatment duration, the proximity of the source with respect to the treated surface, etc., and for treatment of different skin diseases at different dosage levels. Optimization of the source can also be achieved by varying the electrical parameters like applied voltage and frequency.

7.3 Comparison of NO and ozone fluxes with other treatment methods

Flux of NO can be effectively used for healing of wounds. In NO therapy using the 'indirect' air-plasma source 'Plazon', gas mixture in effluent of the plasma source with NO concentration of 500 ppm improved healing of skin wounds (Shekter, 2005). Our DBD plasma source generates comparatively lower NO flux which is too small for similar skin healing treatments. But mechanism of NO therapy is complicated, multifaceted and is far from known yet. The dose of NO-irradiation necessary for therapeutic effect of different diseases is not yet determined. Using simulated species' fluxes, we can determine the time necessary for full coverage of the treated surface by nitric oxide and ozone. Except small regions near the single-filamentary discharges, the treated surface is irradiated by NO and O_3 homogeneously by applying our DBD. The cross section of one molecule amounts $(3\text{-}4)\cdot10^{-20}$ m^2 and therefore, the surface under driving electrode is treated by nitric oxide in about 5 s and by ozone in fraction of a second. In general, for increasing NO production, the averaged current produced in the discharge can be increased. For this, input voltage of higher amplitude or high pulse frequency must be used. A discharge ignited with higher voltages or with higher pulse frequencies can lead to painful medical treatments and so such modifications to the source should be overlooked.

However, the production of NO by the source can be improved by using it at close vicinity to the surface of the human body, thereby reducing the gap distance. Reduced electric field and electron density increase with decrease in the inter-electrode distance. Hence, using the source close to the body can increase the dissociation of nitrogen and oxygen molecules and thus result in effective production of NO. The discharge on the surface of dielectric ignites after the discharge channel bridges the electrodes by operation in single-filamentary mode (Kuchenbecker, 2009). This surface discharge is characterized by relatively high electric field and electron density. The discharge channel on the surface of dielectric is lengthier than that ignited in the air-gap between the electrodes. Therefore, production of NO molecules in the surface discharge is more effective on the dielectric surface than in the air-gap. Also, the flux of NO molecules produced in the surface discharge increases with decreased inter-electrode distance. So, using the source close to the body surface allows the NO molecules produced in the surface discharge to reach the treated surface effectively.

Some chemical active species produced in air plasma e.g. ozone and nitric oxides can be harmful for human body when inhaled but serve useful for medical treatments like treatment of dermatological disorders and healing of wounds. At that, required concentration of these species must be supported near the treated object. An advantage of 'direct' plasma treatment is the production of chemically-active species directly on treated site of human skin. Despite the fact that these species diffuse from the active plasma volume and can reach respiratory tract, their concentration decreases drastically during diffusion and reaches the safety level at small distance away from the active plasma volume.

8. Conclusion and outlook

A DBD is investigated towards medical applications especially for skin treatment. DBD operated on human and animal skin consists of both homogeneous and single-filamentary modes, which are ignited simultaneously. Characterization of this complex discharge appears to be a complicated task. Hence, these two discharge modes namely the single-filamentary and homogeneous modes are studied separately. Single-filamentary discharge is produced with Al-spike as opposite electrode. A homogeneous discharge is obtained with glass as opposite electrode which is typically a Townsend discharge but does not attain a glow mode in our experimental conditions. Using optical emission spectroscopy, microphotography and numerical simulation, the plasma parameters and gas temperature in DBD on mouse are determined, chemical kinetics in active plasma volume and in afterglow is simulated and irradiation of the treated object by ozone, nitric oxide and UV-photons are calculated. These fluxes are compared with other sources used in dermatology. By applying the DBD in single-filamentary mode, irradiation of treated surface reaches a maximum of about 1 $W \cdot m^{-2}$ for both UV-A and UV-B spectral range, and in the homogeneous mode it is about 0.2 $W \cdot m^{-2}$. Irradiation of the treated surface by photons and chemically active particles can be increased simply by increasing the trigger pulse frequency; but electric current will also increase and could evoke pain during treatment. When the DBD is operated in the single-filamentary mode, the flux of nitric oxide and ozone to the treated surface attain a maximum of $4.8 \cdot 10^{19}$ $m^{-2} \cdot s^{-1}$ and $2.2 \cdot 10^{21}$ $m^{-2} \cdot s^{-1}$, respectively. NO flux is about $7 \cdot 10^{18}$ $m^{-2} \cdot s^{-1}$ and ozone flux about $6.6 \cdot 10^{19}$ $m^{-2} \cdot s^{-1}$, when operated in the homogeneous mode.

The presented simulation of chemical kinetics is based on the time and spatial-averaged plasma parameters and can have indefinite systematical error up to factor about 2. To improve accuracy and reliability of the simulation, optical emission diagnostics with time and spatial resolution will be applied in further studies.

To increase surface irradiation of the treated object by active species and UV photons, modified electrode arrangements where the discharge in the gas gap will be supplemented with effective surface discharge on the dielectric will be employed and studied.

9. Acknowledgment

The authors gratefully acknowledge Dr. Ch. Opländer and Prof. Dr. Ch. V. Suschek from Department of Plastic and Reconstructive surgery, Hand surgery and Burn Center (Medical Faculty, RWTH Aachen, Germany) for their valuable help in carrying out the experiment with living mouse. Financial support by German Research Foundation of the project C2 of Research Group FOR 1123 "Physics of Microplasma" is also gratefully acknowledged.

10. References

Ayan, H.; Fridman, G.; Gutsol, A.F.; Vasilets, V.N.; Fridman, A. & Fridman, G. (2008). Nansecond-pulsed uniform dielectric-barrier discharge. *IEEE Trans.Plasma Sci.*, Vol. 36, pp. 504-508

Ayan, H.; Staack, D.; Fridman, G.; Gutsol, A.F.; Mukhin, Y.; Starikovskii, A; Fridman, A. & Fridman, G. (2009). Application of nanosecond-pulsed dielectric barrier discharge

for biomedical treatment of topographically non-uniform surface. *J.Phys.D:Appl.Phys.*, Vol., 42, p. 125202 (5pp)

Bibinov, N.K.; Kokh, D.B.; Kolokolov, N.B.; Kostenko, V.A.; Meyer, D.; Vinogradov, I.P. & Wiesemann, K. (1998). A comparative study of the electron distribution function in the positive columns in N_2 and N_2/He dc glow discharges by optical spectroscopy and probes. *Plasma Sources Sci.Technol.*, Vol. 7, pp. 109-128

Bibinov, N.K.; Bratsev, V.F.; Kokh, D.B.; Ochkur, V.I. & Wiesemann, K. (2005). Spectroscoic determination of the cold electron population in very low pressure ECR discharges in N_2/He mixture. *Plasma Sources Sci.Technol.*, Vol. 14, pp. 298-309

Bibinov, N.; Halfmann, H.; Awakowicz, P. & Wiesemann, K. (2007). Relative and absolute intensity calibrations of a modern broadband echelle spectrometer. *Meas.Sci.Technol.*, Vol. 18, pp. 1327-1337

Bibinov, N.; Halfmann, H. & Awakowicz, P. (2008). Determination of the electro energy distribution function via optical emission spectroscopy and a Langmuir probe in an ICP. *Plasma Sources Sci.Technol.*, Vol. 17, p. 035004(7pp)

Boudam, M.K; Moisan, M,; Saoudi, B.; Popovici, C.; Gherardi, N. & Massines, F. (2006). Bacterial spore inactivation by atmospheric-pressure plasmas in the presence or absence of UV photons as obtained with the same gas mixture. *J.Phys.D:Appl.Phys.*, Vol., 39, pp.3494-3507

Bruch-Gerhurz, D.; Ruzicka, T. & Kolb-Bachofen, V. (1998). Nitric oxide in human skin: Curret status and future prospects. *J. Invest. Dermatol.*, Vol., 110, pp.1-7

Cals-Grierson, M.M. & Ormerod, A. D. (2004). Nitric oxide function in the skin. *Nitric Oxide*. Vo., 10, pp.179-193

Childress, B. B. & Stechmiller, J. K. (2002). Role of nitric oxide in wound healing. *Biological Research for Nursing*, Vol., 4, pp.5-15

Coven, T.R.; Burack, L.H.; Gilleaudeau, P.; Keogh, M.; Ozawa, M. & Kruege, J.G. (1997). Narrowband UV-B produces superior clinical and histological resolution of moderate-to-severe psoriasis in patients compared with broad-band UV-B_2. *Arch.Dermatol.*, Vol., 133, pp.1514-1522

Fridman, G.; Brooks, A.D.; Balasubramanian, M.; Fridman, A.; Gutsol, A.; Vasilets, V.N.; Ayan, H. & Friedman, G. (2007). Comparison of direct and indirect effects of non-thermal atmospheric-pressure plasma on bacteria. *Plasma Proc.Polymer.*, Vol., 4, pp. 370-375

Fridman, G.; Friedman, G.; Gutsol, A.; Shekhter, A.B.; Vasilets, V.N. & Fridman, A. (2008). Applied plasma medicine. *Plasma Proc.Polymer.*, Vol., 5, pp. 503-533

Gibalov, V.I. & Pietsch, G.J. (2000). The development of dielectric barrier discharges in gas gaps and on surfaces, . *J.Phys.D: Appl.Phys.*, Vol., 33, pp. 2618-2636

Godyak, V.A.; Piejak, R.B. & Alexandrovich, B.M. (1992). Measurements of electron energy distribution in low-pressure RF discharges. *Plasma Sources Sci.Technol.*, Vol. 1, pp. 36-58

Halfmann, H.; Denis, B.; Bibinov, N.; Wunderlich, J. & Awakowicz, P. (2007). Identification of the most efficient VUV/UV radiation fo plasma based inactvation of *Bacillus atrophaeus* spores. *J.Phys.D: Appl.Phys.*, Vol., 40, pp. 5907-5911

Hannuksela, M.; Karvonen, J.; Husa, M.; Jokela, R.; Katajamäki, L. & Leppisaari, M. (1985). Ultraviolet light therapy in atopic dermatitis. *Acta.Dermotol.Venerol.Suppl.(Stockh)*, Vol., 114, pp. 137-139

Itikawa, Y.; Ichimura, A.; Onda, K.; Sakimoto, K.; Takayanagi, K.; Hatano, Y.; Hayashi, M.; Nishimura, H. & Tsurubuchi, S. (1989). Cross section for collisions of electron and photons with oxygen molecules. *J.Phys.Chem.Ref.Data* , Vol., 18, pp. 23-42

Itikawa, Y. (2006). Cross section for electron collisions with nitrogen molecules. *J.Phys.Chem.Ref.Data* , Vol., 35, pp. 31-53

Jekler, J. & Larko, O. (1990). Combined UVA-UVB versus UVB phototherapy for atopic dermatitis: A paired-comparison study. *Journal of the American Academy of Dermatology*, Vol., 22, pp. 49- 53

Kishan Kumar, Y.H.; Rao, G.R.R.; Gopal, K.V.T.; Shanthi, G. & Rao K.V. (2009). Evaluation of narrow-band UVB phototherapy in 150 patients with vitiligo. *Indian J.Dermatol.Venerol.Leprol.*, Vol., 75, pp. 162-166

Kogelschatz, U. (2003). Dielectric-barrier discharges. Their history, discharge physics, and industrial applications. *Plasma Chem.Plasma Proc.,* Vol.,23, pp.1-46

Kozlov, K.V.; Wagner, H.-E.; Brandenburg, R & Michel, P. (2001). Spatio-temporally resolved spectroscopic diagnostics of the barrier discharge in air at atmospheric pressure. *J.Phys.D: Appl.Phys.*, Vol., 34, pp. 3164-3176

Krutmann, J.; Chech, W.; Diepgen, T.; Niedner, R.; Kapp, A. & Schoepf, E. (1992). High-dose UVA_1 theraphy in the treatment of patients with atopic dermatitis. *J.Am.Acad.Dermatol*, Vol., 26, pp.225-230

Kuchenbecker, M; Bibinov, N; Kaemlimg, A; Wandke, D.; Awakowicz, P. & Viöl, W. (2009). Characterization of DBD plasma source for biomedical applications. *J.Phys.D:Appl.Phys.*, Vol. 42, p.045212(10pp)

Legrini, O.; Olivers, O. & Braun, A.M. (1993). Photochemical process of water treatment. *Chem.Rev.*, Vol., 93, pp. 671-698

Libermann, M.A. & Lichtenberg, A.J. (1994). *Principles of plasma discharges and materials processing*. John Wiley & Sons Inc.

Massines, F.; Rabehi, A.; Decomps, P; Gadri, R.B.; Segur, P & Mayoux, C. (1998). Experimental and theoretical study of a glow discharge at atmospheric pressure controlled by dielectric barrier. *J.Appl.Phys.*, Vol., 83, pp.2950-2957

Pancheshnyi, S.V.; Starikovskaia, S.M. & Starikovskii A.Yu. (2000). Collisional deactivation of $N_2(C^3\Pi_u, v= 0,1,2,3)$ states by N_2, O_2, H_2 and H_2O molecules. *Chem.Phys.*, Vol., 262, pp. 349-357

Raizer, Y.P. (1997). *Gas discharge physics*, Springer-Verlag, Berlin, Heidelberg, New York

Rajasekaran, P; Mertmann, P; Bibinov, N; Wandke, D.; Viöl, W. & Awakowicz, P. (2009). DBD plasma source operated in single-filamnetary mode for therapeutic use in dermatology. *J.Phys.D:Appl.Phys.*, Vol. 42, p.225201(10pp)

Rajasekaran, P; Mertmann, P; Bibinov, N; Wandke, D.; Viöl, W. & Awakowicz, P. (2010). Filamentary and homogeneous modes of dielectric barrier discharge (DBD) in air: Investigation through plasma characterization and simulation of surface irradation. *Plasma Proc.Polymer.*, Vol. 7, pp. 665-675

Shekter, A.B.; Serezhenkov, V.A.; Rudenko, T.G.; Pekshev, A.V. & Vanin, A.F. (2005). Benefecial effect of gaseous nitric oxide on the healing of skin wounds. *Nitric oxide: Biolo.Chem.*, Vol., 12, pp. 210-219

Stege, H.; Berneburg, M.; Humke, S.; Klammer, M.; Grewe, M.; Grether-Beck, S.; Boedeker, R.; Diepgen, T.; Dierks, K.; Goerz, G. & Rizicka, T. (1997). High-dose UVA_1

radiation therapy for localized scleroderma *J.Am.Acad.Dermatol*, Vol., 36, pp. 938-944

Stoffels, E. (2007). Tissue processing with atmospheric plasmas. *Contrib.Plasma Phys.*, Vol.,47, pp. 40-48

Stefanovic, I.; Bibinov, N. K.; Deryugin, A.A.; Vinogradov, I. P.; Napartovich, A. P. & Wiesemann, K. (2001). Kinetics of ozone and nitric oxides in dielectric barrier discharges in O_2/NO_x and $N_2/O_2/NO_x$ mixtures. *Plasma Sources Sci.Technol.*, Vol., 10, pp. 406-416

Walsh, J.L; Zhi Cao & Kong, M.G. (2008). Atmospheric dielectric-barrier discharges scalable from 1 mm to 1 m. *IEEE Trans.Plasma Sci.*, Vol., 36, pp. 1314-1315

Biomedical Engineering, Trends in Materials Science

Edited by Mr Anthony Laskovski

ISBN 978-953-307-513-6
Hard cover, 564 pages
Publisher InTech
Published online 08, January, 2011
Published in print edition January, 2011

Rapid technological developments in the last century have brought the field of biomedical engineering into a totally new realm. Breakthroughs in materials science, imaging, electronics and, more recently, the information age have improved our understanding of the human body. As a result, the field of biomedical engineering is thriving, with innovations that aim to improve the quality and reduce the cost of medical care. This book is the second in a series of three that will present recent trends in biomedical engineering, with a particular focus on materials science in biomedical engineering, including developments in alloys, nanomaterials and polymer technologies.

InTech Europe
University Campus STeP Ri
Slavka Krautzeka 83/A
51000 Rijeka, Croatia
Phone: +385 (51) 770 447
Fax: +385 (51) 686 166
www.intechopen.com

InTech China
Unit 405, Office Block, Hotel Equatorial Shanghai
No.65, Yan An Road (West), Shanghai, 200040, China
中国上海市延安西路65号上海国际贵都大饭店办公楼405单元
Phone: +86-21-62489820
Fax: +86-21-62489821

IntechOpen